Consistency of DBI-inspired Dinkic Inflation with Observational Data

Rabia Saleem [*]

Department of Mathematics,

COMSATS, Institute of Information Technology Lahore, Pakistan.

Abstract

In this paper, a new kind of inflation model was used, which has the interesting property that its perturbation equation of motion gets a correction of k^4, due to the non-linearity of the kinetic term. Nonetheless, the scale-invariance of the power spectrum remains valid, both in large-k and small-k limits. we investigate in detail the perturbed parameters including slow-roll parameters, number of e-folds, spectral index, the index running and the tensor/scalar ratio in this model, especially on the potential-driven case. The results are compared to the current observational data. In this case, we also discuss the tensor spectrum, which is expected to be tested by the future observations on primordial gravitational waves.

Keywords: Cosmological Perturbations; Slow-roll approximation.
PACS: 98.80.Cq; 05.40.+j.

1 Introduction

In 1981, Guth [1] invented the term "cosmological inflation", a compelling research aspect in modern cosmology. Inflation is an additional idea in hot big-bang (HBB) theory, which is applied on very initial stage of the cosmic evolution. It is supposed that scale of inflation to be long since over and the

---

[*]rabiasaleem@ciitlahore.edu.pk

standard expansion restored, in order to maintain the significant successes, such as the cosmic microwave background radiation (CMBR) and nucleosynthesis. Regardless of all of its triumphs, there are some unsatisfactory issues with HBB theory which cultivated inflation [2].

The first issue is the "flatness problem" (an easiest one to understand): for flat universe, $\Omega = 1$ on the time scale (where $\Omega = \frac{\rho}{\rho_c}$; ρ_c is the critical density). In standard big-bang model, the curvature term $(aH)^2$ (a, H be the scale factor and Hubble parameter) always a decreasing function of time leading to $\Omega(t)$ different from unity due to cosmic expansion. However, according to recent observations, the value of $\Omega(t)$ is near to unity, thus it must be same (very close to one) in the early-time. For example, its value at *Planck time* is "$|\Omega(t_{Pl})| < \mathcal{O}(10^{-64})$" while "$|\Omega(t_{nucleo})| < \mathcal{O}(10^{-16})$" (during *nucleosynthesis*). These values represent that there was a need of highly fine-tuning of "initial conditions". The inaccurate choice of "initial conditions" leads to the cosmos which either soon expands before the formation of structure or quickly collapses. This dubbed as "flatness problem" [3].

The "horizon problem" illustrate that "Why the temperature of CMBR appears the same in all directions?" In east and west directions, the exactly same temperature of CMBR is detected, while the radiation coming from the east and west are detached by "28 billion light years". As we know that information always transformed with a speed less than the "speed of light", hence neither the radiation detected from two directions of the the universe could be in thermal contact nor the regions ever have been in link. The only possibility for two regions to be in thermal equilibrium is that they must be enough close to communicate with each other. Then, how thermal equilibrium between two regions was attained if there was no causal connection? [3].

The mechanism of inflation is proposed to resolve the standard shortcomings of HBB model. "Stripped to its bare bones", inflation is an era of the cosmic evolution where the scale factor $a(t)$ was growing exponentially ($\ddot{a} < 0$). The acceleration equation immediately implies that "$\rho + 3P < 0$", since density is always assumed positive, so to satisfy the inequality, pressure should be negative ($P < -\frac{\rho}{3}$). Fortunately, the symmetry breaking (concept of modern particle physics) give ways through which this negative pressure can be achieved. A cosmos possessing (Λ) (the cosmological constant, representing by $P = -\rho$) is one of the typical example of inflationary cosmic expansion. After a passage of time, the energy of Λ decayed into ordinary

2

matter which leads to a "graceful exit" from inflation and again preserve the HBB model. Unfortunately, Λ is proved to be a very ad hoc technique. A successful inflationary model must possesses a feasible hypothesis for the source of Λ and a "graceful exit" from the inflation [4].

The "phase transitions" is a basic idea to obtain inflation. This is especially a dramatic event in the cosmic time-line, a time when universe really changes its properties. It is fact that the current cosmos have passed through a series of phase transitions as it cooled down. A curious form of matter named scalar field is consider to be responsible for the cosmic phase transitions. It possesses negative pressure (an effective Λ) and satisfy the condition $(p + 3p < 0)$, necessary to attain inflation. At the end of phase evolution, the inflaton (scalar particle which produced inflation) decomposed and the inflation terminates, hopefully having attained the required cosmic expansion (by a factor of 10^{27} or more).

Inflation resolves the "flatness problem" as: "consider a balloon being very quickly blown up (say to the size of the sun), its surface would then look flat to us. The crucial difference between inflation and the standard HBB model is that the size of the region of the observable universe (given roughly by the "Hubble length" (cH^{-l}; H^{-l} be the age of the universe and c be the maximum speed), does not change while this happens. So, soon you are unable to notice the curvature of the surface. While in the big bang scenario the distance you can see increases very rapidly than the balloon expands, so you can observe more of the curvature as time goes by." The solution of the "horizon problem" can be described in a precise way as: "inflation enlarges the size of a portion of the cosmos, while keeping its peculiar scale (the Hubble scale) fixed. This statement yields that a small patch of the universe, will be small enough to obtain thermal contact before inflation, can expand to be much larger than the size of our presently observable universe. Then the CMBR coming from opposite sides of the sky really are at the same temperature because they were once in equilibrium. Equally, this provides the opportunity to generate irregularities in the universe which can lead to structure formation" [4].

The oscillatory (cyclic) universe have a long past in the field of cosmology [5]. Formerly, one of their basic interest was that the initial conditions could in principle be evaded. However, a detailed analysis of such models affirmed severe problems in their development in the framework of general relativity (GR). Aside from entropy constraints that reduced the number of bounces in the early time, the basic difficulty is the classical treatment when any

bounce is singular, thereby leading to the failure of GR. Current progress in M-theory inspired braneworld models have reborn interest in cyclic (oscillatory) universe, despite the fact, problems still attached with these models in constructing a successful analysis of the bounce [6]. An oscillating universe that subsequently underwent an inflationary cosmic expansion after a finite number of cycles has also been discussed [7]. Yet, a physical method to bring about the bounces was not implemented in this model.

Damour and Mukhanov [8] are the pioneers of "oscillating inflation". They proposed that, after the slow-roll, inflation may lasts in rapid coherent oscillation during the reheating regime. Liddle and Mazumder [9] formulated the corresponding "number of e-folds". The decay of scalar fields in the oscillations to inflaton was also discussed briefly by Bartruma et al. [10]. The adiabatic perturbation in the oscillatory inflation are investigated in [11]. The authors in [12] extended the work of Damour and Mukhanov [8], by taking a coupling between the Ricci scalar curvature and inflaton. An important form of the potential, which is needed to end the oscillatory inflation, was formulated in [13]. The rapid oscillatory phase gives a less "number of e-folds", so it is not possible to avoid the slow-roll phase during this formalism. Because of few "number of e-folds", a deep analysis of the growth of quantum fluctuations has not been executed. To solve this difficulty, we can assume a "non-minimal derivative coupling model". A mess of literature exists to study the cosmological aspects of this model [14].

The oscillatory inflation with "non-minimal kinetic coupling" is presented in [15] which solves the issue of few number of e-folds coming in [8] ("non-minimal derivative coupling model") as it increases the "number of e-folds" during high-friction era. However, it is not clear from this scenario how reheating occurs or the universe becomes radiation dominated after the end of inflation. Sadjadi and Goodarzi [15] analyzed the compatibility of the perturbed parameters like scalar(tensor) perturbations, power spectra and spectral index for scalar(tensor) modes in oscillatory inflation with Planck 2013 data. The isotropic universe is just an perfect realization to the cosmos we observe as it ignores all the structure and other observed anisotropies, e.g., in the CMB temperature [16]. One of the great triumphs of inflation is to have a naturally embedded mechanism to account for these anisotropies. Sharif and Saleem [17] studied warm vector inflation in "locally rotationally symmetric Bianchi type I" (LRS BI) universe model and verified its compatibility with WMAP7 data.

Motivated by the combined work of Sadjadi and Goodarzi [15], I have

discussed inflationary scenario during rapid oscillation of a scalar field in non-minimal derivative coupling model. To this end, the framework of LRS BI universe model is used. The paper is organized as follows. The basic formalism of oscillatory inflation in the background of LRS BI universe model is given in section **2**. Section **3** deals with cosmological perturbations during minimal and non-minimal cases. I evaluate explicit expressions for perturbed parameters and analyzed them through graphical trajectories by constraining the model parameters with Planck 2015 observations. Finally, the results are concluded in the last section.

2 Formalism of Anisotropic oscillatory Inflation

In the past three decades, various inflationary models have been proposed, where in many of them inflation is driven by a canonical scalar field (ϕ), rolling slowly in an almost flat potential. Higgs boson is considered to be a natural candidate for inflaton [18]. Inspired by this idea, Germani and Kehagias [19] introduced a non-minimal coupling between kinetic term of ϕ and the Einstein tensor ($G^{\mu\nu}$), tried to consider the inflaton as the Higgs boson, without violating the unitarity bound. This model is specified by the following action

$$S = \int \left(\frac{M_P^2}{2} R - \frac{1}{2} \Delta^{\mu\nu} \partial_\mu \phi \partial_\nu \phi - V(\phi) \right) \sqrt{-g} d^4 x,$$

where $\Delta^{\mu\nu} = g^{\mu\nu} - \frac{1}{M^2} G^{\mu\nu}$ (M be a coupling constant with dimension of mass, $G^{\mu\nu} = R^{\mu\nu} - \frac{1}{2} R g^{\mu\nu}$) and $M_P = 2.435 \times 10^{18} GeV$ is the reduced Planck mass. I have considered the gravitational enhanced friction model in the framework of LRS BI model. The model is represented by the following line element

$$ds^2 = -dt^2 + a^2(t) dx^2 + b^2(t)(dy^2 + dz^2),$$

with $a(t)$, $b(t)$ are the scale factors along x-axis and (y, z)-axis, respectively. This metric can be transformed in the following form using a linear relationship $a = b^m$, $m \neq 1$ [20]

$$ds^2 = -dt^2 + b^{2m}(t) dx^2 + b^2(t)(dy^2 + dz^2).$$

The equation of motion for inflaton is given as

$$\left(1 + (m+2)\frac{H_2^2}{M^2}\right)\ddot{\phi} \ + \ (m+2)H_2\left(1 + (m+2)\frac{H_2^2}{M^2} + (m+2)\frac{2\dot{H}_2}{3M^2}\right)\dot{\phi}$$
$$= \ -V'(\phi), \tag{1}$$

where $H_2 = \frac{\dot{b}}{b}$, $V(\phi)$ are the directional Hubble parameter and the effective potential, respectively. Dot and prime represent the derivative with respect to time and scalar field. The energy density (ρ_ϕ) and the pressure (P_ϕ) for homogeneous and anisotropic scalar field can be expressed as, respectively

$$\rho_\phi \ = \ \left(1 + (m+2)^2\frac{H_2^2}{M^2}\right)\frac{\dot{\phi}^2}{2} + V(\phi),$$
$$P_\phi \ = \ \left(1 - (m+2)\frac{H_2^2}{M^2} - (m+2)\frac{2\dot{H}_2}{3M^2}\right)\frac{\dot{\phi}^2}{2} - \frac{2(m+2)}{3M^2}\dot{\phi}\ddot{\phi} - V(\phi).$$
$$\tag{2}$$

The dynamics of anisotropic oscillatory inflation is described by the evolution equation given by

$$H_2^2 = \frac{1}{(1+2m)M_P^2}\rho_\phi. \tag{3}$$

Here, I consider the rapid oscillatory solution for ϕ, with both time dependent amplitude $\Phi(t)$ (the highest point of oscillation at which $\dot{\phi} = 0$) and frequency $\omega(t) = \frac{1}{T(t)}$, where $T(t)$ (the period of oscillation) is defined as

$$T = 2\int_{-\phi}^{\phi}\frac{d\phi}{\dot{\phi}}. \tag{4}$$

The rapid oscillation phase obeys the following conditions

$$H_2(t) \ll \frac{1}{T(t)}; \quad |\frac{\dot{H}_2}{H_2}| \ll \frac{1}{T(t)}, \tag{5}$$

implying that the directional Hubble parameter changes insignificantly during one oscillation (i.e., $H_2(t') \approx H_2(t)$ for $t \leq t' \leq t + T(t)$). Equations (3) and (5) together yield that similar to H_2, ρ_ϕ also remains approximately constant during one period. We take the constant value of inflaton density

6

at the amplitude, Φ (where $\dot{\phi}\mid_{|\phi|=\Phi}=0$). Therefore ρ_ϕ during one oscillation can be expressed in terms of $V(\phi)$ as $\rho_\phi = V(\phi)$ at the corresponding Φ [21].

Therefore, for a power law potential, I expect that $|\frac{\dot{\phi}}{\phi}| \ll \frac{1}{T}$. To elucidate more this subject, the rapid oscillating scalar field is depicted numerically using Eqs.(1)-(3) for a quadratic potential, showing that the amplitude of oscillation changes very slowly during one oscillation. Also in Fig. **1**, the oscillation of the scalar field for the potential $V(\phi) = \lambda|\phi|^q$ is numerically shown for $q \in (-2, \infty)$ (the reason for this choice will be revealed when we will determine our parameters from astrophysical data in the third section).

The adiabatic index (γ) is related with equation of state (EoS) parameter ($w = \frac{P_\phi}{\rho_\phi}$) as $w = w + 1$. In the rapid oscillation phase, it can be calculated using Eqs.(3), (4) and the expression $\rho_\phi = V(\phi)$ as follows

$$
\begin{aligned}
\gamma &= \frac{\langle P_\phi + \rho_\phi \rangle}{\langle \rho_\phi \rangle} = \frac{1}{\langle \rho_\phi \rangle}\left[\left(1 + \frac{(m+2)^2 H_2^2}{3M^2}\right)\langle \dot{\phi}^2 \rangle - \frac{d}{dt}\left(\frac{(m+2)H_2\dot{\phi}^2}{3M^2}\right)\right], \\
&= \left(1 + \frac{(m+2)^2 H_2^2}{3M^2}\right)\frac{\langle \dot{\phi}^2 \rangle}{\langle \rho_\phi \rangle} = \frac{2\left(1 + \frac{(m+2)^2 H_2^2}{3M^2}\right)}{\left(1 + \frac{(m+2)^2 H_2^2}{M^2}\right)}\frac{\langle \rho_\phi - V(\phi) \rangle}{\langle \rho_\phi \rangle}, \\
&= \frac{2\left(1 + \frac{(m+2)^2 H_2^2}{3M^2}\right)}{\left(1 + \frac{(m+2)^2 H_2^2}{M^2}\right) V(\Phi)}\frac{\int_{-\phi}^{\phi}\sqrt{V(\Phi) - V(\phi)}}{\int_{-\phi}^{\phi}\frac{d\phi}{\sqrt{V(\Phi)-V(\phi)d\phi}}},
\end{aligned}
\tag{6}
$$

where the bracket $\langle \cdots \rangle = \frac{\int_t^{t+T}\cdots dt'}{T}$ denotes the time averaging. To obtain above equation, it is taken into account the fact that $\dot{\phi}$ vanishes at $\mid \phi \mid= \Phi$. Using power law potentials of the form $V(\phi) = \lambda\phi^q$ ($\lambda \in \mathcal{R}$), one can easily obtained the average adiabatic index as

$$
\gamma = \frac{2q}{q+2}\left(\frac{1 + \frac{(m+2)^2 H_2^2}{3M^2}}{1 + \frac{(m+2)^2 H_2^2}{M^2}}\right),
\tag{7}
$$

where q is a dimensionless real parameter, while the limit $q \to 0$, gives a logarithmic potential. In the minimal coupling case ($M \to \infty$), the adiabatic index reduced to $\gamma = \frac{2q}{q+2}$. In the high friction regime, where $\frac{H_2^2}{M^2} \gg 1 \Rightarrow \gamma = \frac{2q}{3q+6}$.

The average rate of change of ρ_ϕ is given as

$$
\langle \dot{\rho}_\phi \rangle = \lim_{T\to 0}\frac{\rho_\phi(t+T) - \rho_\phi(t)}{T} \simeq \dot{\rho}_\phi.
\tag{8}
$$

7

By taking the average of the continuity equation, we obtain

$$\langle \dot{\rho}_\phi + (m+2)H_2(\rho_\phi + P_\phi) \rangle = \dot{\rho}_\phi + (m+2)H_2\gamma\rho_\phi = 0, \tag{9}$$

where γ is given in Eq.(6). For constant γ, the Eqs.(3) and (9) can be solved analytically. For the situation $\frac{H_2^2}{M^2} \gg 1$, the analytical solutions for ρ_ϕ, $b(t)$ and $H_2(t)$ are as follows, respectively

$$\rho_\phi \propto b^{-(m+2)\gamma}, \quad b \propto t^{2/(m+2)\gamma}, \quad H_2 = \frac{2}{(m+2)\gamma t}. \tag{10}$$

Next, I restrict the work to the high friction regime to find out the analytical solution of the model. In the case of power law potential, the period is calculated by the following formula

$$
\begin{aligned}
T &= 2\int_{-\Phi}^{\Phi} \frac{d\phi}{\dot{\phi}}, \\
&= 2\sqrt{\frac{(m+2)H_2^2}{2M^2}} \int_{-\Phi}^{\Phi} \frac{1}{\sqrt{\rho_\phi - V(\phi)}} d\phi, \\
&= 2\sqrt{\frac{(m+2)H_2^2}{2M^2}} \int_{-\Phi}^{\Phi} \frac{1}{\sqrt{\lambda\Phi^q - \lambda\phi^q}} d\phi, \\
&= 2\sqrt{\frac{\pi(m+2)}{2M^2\lambda}} \frac{\Gamma(\frac{1}{q})}{q\Gamma(\frac{q+2}{2q})} H_2 \Phi^{\frac{2-q}{2}}, \\
&= \frac{2}{MM_p}\sqrt{\frac{\pi(m+2)}{2(1+2m)}} \frac{\Gamma(\frac{1}{q})}{q\Gamma(\frac{q+2}{2q})} \Phi, \tag{11}
\end{aligned}
$$

where $H_2 = \sqrt{\frac{\lambda}{(1+2m)}} \frac{\Phi^{\frac{q}{2}}}{M_p}$. The condition, $H_2 T \ll 1$, can be rewritten in terms of inflaton using above two expressions as

$$\Phi^{\frac{q+2}{2}} \ll \frac{MM_p^2(1+2m)q}{\sqrt{2\pi\lambda(m+2)}} \frac{\Gamma(\frac{q+2}{2q})}{\Gamma(\frac{1}{q})}, \tag{12}$$

where the scale M present in the above expression reduces the scale of ϕ as compared to the minimal case, which gives

$$\Phi \ll \frac{\sqrt{(1+2m)}q}{\sqrt{2\pi(m+2)}} \frac{\Gamma(\frac{q+2}{2q})}{\Gamma(\frac{1}{q})} M_p. \tag{13}$$
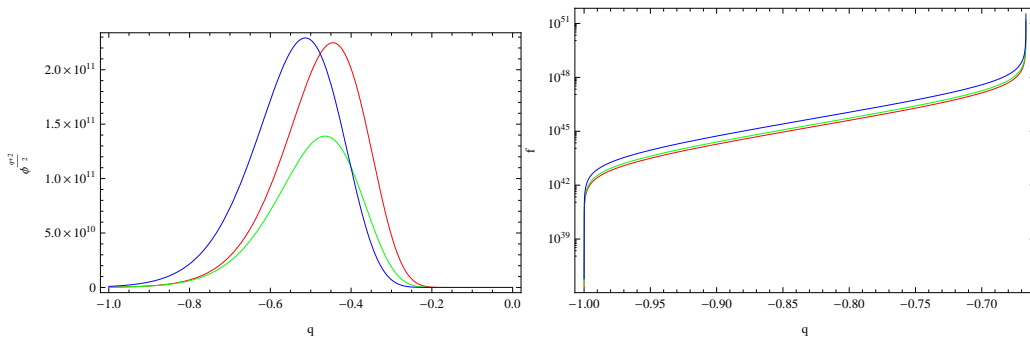
8

Figure 1: (left) The behavior of $\phi^{\frac{q+2}{2}}$ versus q; (right) f versus q are plotted for $m = 1.5$ (red); $m = 2.5$ (green); $m = 10$ (blue).

Therefore, the evaluated solution must be valid in the domain of Eq.(12) which specifies a bound for H_2 and consequently for ρ_ϕ during rapid oscillation. In order to check, either the inequality given in Eq.(12) holds or not, we have plotted Fig.**1**. The left term, $\Phi^{\frac{q+2}{2}}$ and expression on right hand side (say f) of Eq.(12) are plotted versus q, for specified values of m, in the left and right panel of Fig.**1**, respectively. It is very much clear from the comparison of left and right graph of Fig.**1** that the value of $\Phi^{\frac{q+2}{2}}$ is much less than the expression f for $q < 2$ and $m > 1$.

The slow-roll conditions, $\ddot{\phi} \ll (m+2)H_2\dot{\phi}$ and $\rho_\phi \approx V(\phi)$ together with the expression of ρ_ϕ given in the first equation of Eq.(2) generates the following inequality

$$\left(1 + \frac{(m+2)^2 H_2^2}{M^2}\right) \frac{\dot{\phi}^2}{2} \ll V(\phi). \tag{14}$$

In high friction regime ($\frac{H_2^2}{M^2} \gg 1$), all the above mentioned conditions are satisfied when $\phi^{q+2} \gg \frac{q^2 M^2 M_p^4}{\lambda}$ (opposite to Eq.(12)) holds. Equation (14) leads to

$$\frac{(m+2)^2 H_2^2}{2M^2} \dot{\phi}^2 \ll V(\phi) \sim (1+2m)M_p^2 H_2^2, \tag{15}$$

resulting that

$$\dot{\phi}^2 \ll \frac{2(1+2m)}{(m+2)^2} M^2 M_p^2. \tag{16}$$

While during quasi periodic regime, Eqs.(3) and (6) produce the expression $\langle \dot{\phi}^2 \rangle \approx \gamma M^2 M_p^2$.

9

Inflation takes place when $\ddot{b} > 0$ or equivalently $\gamma < \frac{2}{3}$, putting in the expression of γ, I can fix a range of $q \in (-2, \infty)$. While during the minimal case ($\gamma = \frac{2q}{q+2}$), inflation occurs only for the short interval $q \in (-2, 1)$. As already mentioned that the inflation continues as long as $\gamma < \frac{2}{3}$, then fourth equality of Eq.(6) produces

$$\left(\frac{1 + \frac{(m+2)^2 H_2^2}{3M^2}}{1 + \frac{(m+2)^2 H_2^2}{M^2}} \right) \langle \rho_\phi - V(\phi) \rangle < \frac{1}{3} \langle \rho_\phi \rangle. \tag{17}$$

The above expression leads to constraint the potential in high friction and minimal regimes as, respectively

$$\frac{H_2^2}{M^2} \gg 1 \Rightarrow \langle V(\phi) \rangle \gg 0, \quad \frac{H_2^2}{M^2} \to 0 \Rightarrow \langle V(\phi) \rangle > \frac{2}{3} \langle \rho_{(\phi)} \rangle.$$

Inflation ends also for more complicated potential such as the potential suggested by Damour-Mukhanov [8]

$$V(\phi) = \nu \left(\left(\frac{\phi^2}{\phi_c^2} + 1 \right)^{\frac{q}{2}} - d \right), \tag{18}$$

where $d > 0$ is a dimensionless real number while ν, ϕ_c are real parameters with dimensions $[mass]^4$ and $[mass]$, respectively. For $\phi \gg \phi_c$, the above potential reduced to simple power law potential.

The average potential can be evaluated by the following formula [22]

$$\langle V(\phi) \rangle = \frac{\int_{-\Phi}^{\Phi} \frac{V(\phi)}{\dot{\phi}} d\phi}{\int_{-\Phi}^{\Phi} \frac{d\phi}{\dot{\phi}}},$$

leads to find that the inflation continues as long as $\int_{-\Phi}^{\Phi} V(\phi) d\phi > 0$. For the potential, given in Eq.(18), we have

$$\int_{-1}^{1} ((\mathfrak{b}^2 \chi^2 + 1)^{\frac{q}{2}} - d) d\chi > 0, \tag{19}$$

here, $\mathfrak{b} = \frac{\Phi}{\phi_c}$ and $\chi = \frac{\phi}{\Phi}$. The above equation results in that the inflation continues whenever $d < g(\mathfrak{b}, q)$, where

$$g(\mathfrak{b}, q) = \frac{G(\mathfrak{b}, q)}{2\mathfrak{b}\Gamma(\frac{q+3}{2})(1+q)\Gamma(-\frac{q}{2})}, \tag{20}$$

$$G(\mathfrak{b}, q) = -\pi^{\frac{3}{2}}(q+1)sec(\frac{\pi q}{2})_2F_1(-\frac{q}{2}; -\frac{1+q}{2}; \frac{1-q}{2}; -\mathfrak{b}^{-2})\Gamma(-\frac{q}{2})\Gamma(-\frac{q+3}{2}),$$
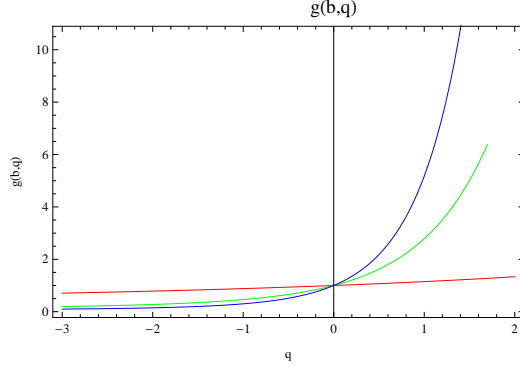
10

Figure 2: $g(\mathfrak{b}, q)$ versus q: for $\mathfrak{b} = 1$ (red); $\mathfrak{b} = 5$ (green); $\mathfrak{b} = 10$ (blue).

where $_2F_1$ is the Gauss hypergeometric function. When this inequality is violated (such that $d = g(\mathfrak{b}_{end}, q)$ and $d > g(\mathfrak{b}(t > t_{end}), q))$, inflation ceases at t_{end}. The graphical analysis of the function is shown in Fig. **2** for three different values of $\mathfrak{b} = 1$, 5, 10. It is observed that $g(\mathfrak{b}, q)$ has an increasing behavior for all values of $\mathfrak{b} > 0$ in the range $q \in (-\infty, 1)$ (in agreement with the recent values of the parameters evaluate in the next section). The point of intersection of the three curves is $(1, 0)$, so inflation ends for $d > 1$ and $d \simeq 1$ ($\phi \sim \phi_c$).

The number of e-folds $(\mathcal{N})$ from a specific time (t_*) until the end of inflation (t_{end}) can be defined as [9]

$$\mathcal{N} = \ln \frac{b_{end} H_{2end}}{b_* H_{2*}}, \tag{21}$$

here, $\mathcal{N}$ is a measure of $\ln(bH_2)$, increases during inflation. Substituting the expressions of scale factor and directional Hubble parameter from Eq.(10), we arrive at

$$\mathcal{N} = \frac{q}{2} \left(\frac{2}{(m+2)\gamma} - 1 \right) \ln \frac{\phi_*}{\phi_{end}}. \tag{22}$$

During high friction and minimal regimes, the above expression turns out to be as

$$
\begin{aligned}
\mathcal{N} &= \frac{3}{2} \left(\frac{q - m}{m + 2} \right) \ln \left(\frac{\phi_*}{\phi_{end}} \right), \\
\mathcal{N}_{min} &= \left(\frac{q - 2m - 2}{2(m + 2)} \right) \ln \left(\frac{\phi_*}{\phi_{end}} \right),
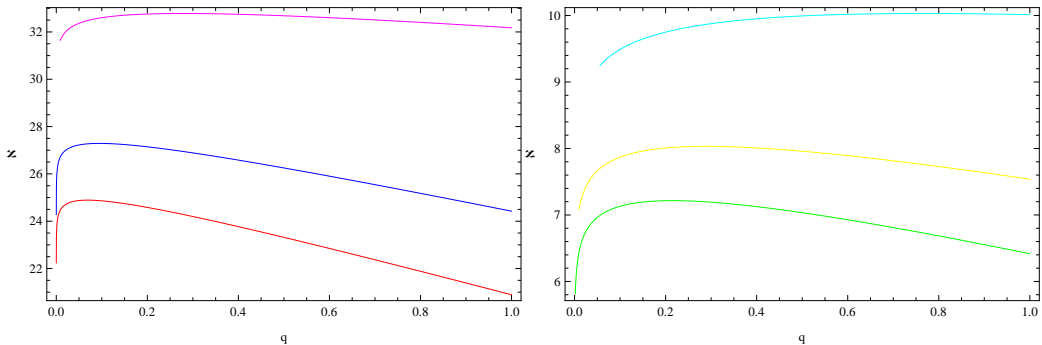\end{aligned}
\tag{23}
$$

11

Figure 3: (left) $\mathcal{N}$ versus q for $\Phi_{end} \sim 10^{-17}m_P$, $m = 1.1$ (red); $m = 2.5$ (blue); $m = 10$ (purple); (right) $\mathcal{N}$ versus q for $\Phi_{end} \sim 10^{-6}m_P$, $m = 1.1$ (green); $m = 2.5$ (yellow); $m = 10$ (cyan).

respectively. On comparing, we can note that our considered model has more number of e-folds as compared to $\mathcal{N}_{min}$ with a common term $\ln\left(\frac{\phi_*}{\phi_{end}}\right)$. During intermediate regime (where high friction condition violates), we can not obtain feasible solution for b and H_2, hence unable to conclude a simple form for $\mathcal{N}$.

Now, we specify a lower bound for $\mathcal{N}$ during inflation. Let us take t_k be the time where $\lambda_k = \frac{1}{k}$ (length scale), attributed to the wavelength $k = \frac{1}{\lambda_k} = b(t_k)H_2(t_k)$ (where $b(t_0) = 1$ and t_0 be the present time), exited the Hubble radius during inflation. The LSS observations are limited to scales of about $1Mpc$ (denoted by λ_{min}) to the present Hubble radius (λ_{max}). These observable scales crossed the Hubble radius during the following visible e-folding

$$\mathcal{N}_{vis} = \ln\left(\frac{\lambda_{max}}{\lambda_{min}}\right) = \ln\left(\frac{H_0^{-1}}{1Mpc}\right). \tag{24}$$

Putting $H_0 = 67.3km/sMpc^{-1}$ ($95\%C.L.$) [23], we obtain $\mathcal{N}_{vis} = 8.4$. Hence, all relevant scales exited the Hubble radius during 8.4 e-folding after $\frac{1}{H_0}$'s exit, so $\mathcal{N} > 8.4$. Equations (13) and (23) lead to following e-folding number during minimal case

$$\mathcal{N}_{min} < \left(\frac{q - 2m - 2}{2(m + 2)}\right) \ln\left(\left(\frac{\sqrt{2(1 + 2m)}}{2\sqrt{\pi(m + 2)}} \frac{q\Gamma(\frac{q+2}{2q})}{\Gamma(\frac{1}{q})}\right) \frac{M_P}{\phi_{end}}\right),$$

where ϕ_{end} depends on the chosen potential (given in Eq.(18)). For instance, Φ_{end} is of the same order of ϕ_c for $d = 1$ in Eq.(18). To set an upper bound

12

on $\mathcal{N}_{min}$, I have plotted trajectories for $\mathcal{N} - q$ taking Φ_{end} is equivalent to electroweak scale, i.e., $\Phi_{end} \sim 10^{-17} m_P$ (m_P be the planck mass) (left panel) and $\Phi_{end} \sim 10^{-6} m_P$ (right panel) and varying $m = 1.5,\ 2.5,\ 10$ in Fig.**3**. It is noticed from both graphs of Fig.**3** that an increment in the scale of Φ_{end} leads to decrease the value of $\mathcal{N}_{min}$. An increasing relationship also observed between $\mathcal{N}$ and m. The electroweak scale sets an upper bound, i.e., $\mathcal{N}_{min} < 24$ ($m = 1.5$), $\mathcal{N}_{min} < 26$ ($m = 2.5$), $\mathcal{N}_{min} < 32$ ($m = 10$) while $\mathcal{N}_{min} < 7$ ($m = 1.5$), $\mathcal{N}_{min} < 8$ ($m = 2.5$), $\mathcal{N}_{min} < 10$ ($m = 10$) for $\Phi_{end} \sim 10^{-6} m_P$. The theory may become more viable at least in the context of perturbations generation as the anisotropic model has ability to provide more number of e-folds ($\mathcal{N} > 8.4$) in non-minimal case as compared to the minimal case.

Again considering the scale $k = \frac{1}{\lambda_k} = b(t_k) H_2(t_k)$, a wave-number had chance to exit the Hubble radius during rapid oscillatory phase, following the condition $k \ll \frac{1}{T(t_k)}$ ($H_2 T \ll 1$; $b(t_0) = 1$). To examine this condition, we proceed as that the maximum scale of our observable universe is of the same order of magnitude as $\lambda_{max} = \frac{1}{H_2}$. Since an upper bound for period T can be determined using last equality of Eq.(11) and Eq.(13) during rapid oscillation: $T(t) < T_u$. Therefore, $H_2 T_u \ll 1$ guarantees the consistency of our assumptions with the horizon exit of λ_{max} during rapid oscillation era. This can be elaborated as

$$H_2 < \left(\frac{q - 2m - 2}{2(m+2)} \right) \ln \left(\frac{\sqrt{2(1+2m)}}{2\sqrt{\pi(m+2)}} \frac{q\Gamma(\frac{q+2}{2q})}{\Gamma(\frac{1}{q})} \right) \frac{M_P}{\phi_{end}}. \tag{25}$$

If the anisotropic model provides enough e-folds ($N > N_{vis}$) after this exit, also holds the above constraint, then, we can claim that other large cosmological observable scales had also the possibility to exit the Hubble radius during this stage of inflation. Next, I will study perturbations generation and check model parameter's compatibility based on recent astrophysical data.

3   Anisotropic Cosmological Perturbations

In order to study the scalar and the tensor fluctuations, I decouple the space-time into two components: the background and the perturbations. Further, I have considered homogeneous and anisotropic LRS BI background corresponding to the rapid oscillatory inflation in the context of non minimal derivative coupling model studied in the last section. The Mukhanov-Sasaki

equation is used in order to analyze the quantum perturbations in rapid oscil-lation era. This equation, for scalar and tensor perturbations in non-minimal derivative coupling model, is written as follows [24]

$$\frac{d^2 v_{(s,t)}k}{d\eta^2} + \left(c^2_{(s,t)}k^2 - \frac{1}{z_{(s,t)}}\frac{d^2 z_{(s,t)}}{d\eta^2} \right) v_{(s,t)}k = 0, \tag{26}$$

where c_s, c_t are the speed of sound associated with scalar and tensor modes, respectively. The other terms involved in the above equation like the confor-mal time (η) and z_s, z_t are defined as follows

$$
\begin{aligned}
\eta(t) &= \int^t \frac{dt'}{b^{\frac{m+2}{3}}(t')}, \quad z_s = b^{\frac{m+2}{3}}(t) \left(\frac{3}{m+2} \right) \frac{M_p \xi}{H_2} \sqrt{2\Sigma}, \\
z_t &= b^{\frac{m+2}{3}}(t) M_p \sqrt{1-\alpha} \frac{\sqrt{e_{ij}^\lambda e_{ij}^\lambda}}{2},
\end{aligned}
\tag{27}
$$

where

$$\xi = \frac{1-\alpha}{1-3\alpha}, \quad \Sigma = M^2\alpha \left[1 + \frac{(m+2)^2 H_2^2}{3M^2} \left(\frac{1+3\alpha}{1-\alpha} \right) \right].$$

Further,

$$\alpha = \frac{\dot{\phi}^2}{2M^2 M_p^2}, \quad c_s^2 = \frac{(m+2)^2 H_2^2}{9\xi^2\Sigma}\epsilon_s, \quad c_t^2 = \frac{1+\alpha}{1-\alpha},$$

where ϵ_s is given by

$$
\begin{aligned}
\epsilon_s &= \frac{1}{b^{\frac{m+2}{3}}(t)}\frac{d}{dt}\left[\frac{b^{\frac{m+2}{3}}(t)\xi}{\left(\frac{m+2}{3}\right)H_2}(1-\alpha) \right] - (1+\alpha), \\
&= \left(\frac{3}{m+2} \right)\frac{(1-\alpha)^2}{(1-3\alpha)}\left(1 - \frac{\dot{H}_2}{H_2^2} \right) - (1+\alpha). \tag{28}
\end{aligned}
$$

Germani et al. [25] studied Mukhanov-Sasaki equation for quasi-de Sitter background during slow-roll regime, where $\alpha = 0$. Since during rapid oscilla-tion stage, $b(t)$ is a power law function of time, therefore $\epsilon_s = -\left(\frac{3}{m+2}\right)\frac{\dot{H}_2}{H_2^2} \approx \frac{q}{q+2}$. The second equality (constant ϵ_s) is obtained using previous relation-ship of H_2 in terms of γ (given in Eq.10). The expressions for c_s and c_t in

14

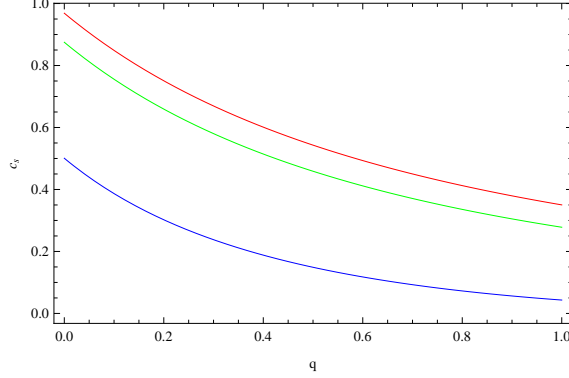Figure 4: Variations in c_s versus q: for $m = 1.1$ (red); $m = 2.5$ (green); $m = 10^3$ (blue).

terms of q can be calculated using ξ, Σ as follows

$$c_s^2 = \frac{(1-3\alpha)^2}{3\alpha(1-\alpha)(1+3\alpha)}\epsilon_s = \frac{\left(1 - \left(\frac{1+2m}{m+2}\right)\left(\frac{q}{q+2}\right)\right)^2}{\left(\frac{1+2m}{m+2}\right)\left(1 - \left(\frac{1+2m}{m+2}\right)\left(\frac{q}{3q+6}\right)\right)\left(1 + \left(\frac{1+2m}{m+2}\right)\left(\frac{q}{q+2}\right)\right)},$$

$$c_t^2 = \frac{q(5m+7) + 6(m+2)}{q(m+5) + 6(m+2)}. \tag{29}$$

From first equality of the above equation, it is noticed that c_s is also constant like ϵ_s. Figure **4** shows that the speed of sound lies in the range $0 < c_s < 1$ for all values of $m > 0$. In the rapid oscillation era, using ξ, Σ, H_2 in z_s, we get

$$z_s = b^{\frac{m+2}{3}}(t)M_p\left(\frac{1-\alpha}{1-3\alpha}\right)\left(\frac{3}{m+2}\right)\sqrt{\frac{2\alpha(m+2)^2(1+3\alpha)}{3(1-\alpha)}}. \tag{30}$$

Since scale factor can be written in terms of conformal time as $b(\eta) \propto \eta^{-\left(\frac{3q+6}{2(m+2)}\right)}$, therefore, $z_{(s,t)} = \beta_{(s,t)}b(\eta)$ where

$$\beta_s = M_p\frac{\left(1 - \left(\frac{1+2m}{m+2}\right)\left(\frac{q}{3q+6}\right)\right)}{\left(1 + \left(\frac{1+2m}{m+2}\right)\left(\frac{q}{q+2}\right)\right)}\sqrt{\frac{2(m+2)(1+2m)\left(\frac{q}{3q+6}\right)\left(1 + \left(\frac{1+2m}{m+2}\right)\left(\frac{q}{q+2}\right)\right)}{3\left(1 - \left(\frac{1+2m}{m+2}\right)\left(\frac{q}{q+2}\right)\right)}},$$

$$\beta_t = M_p\sqrt{1 - \left(\frac{1+2m}{m+2}\right)\left(\frac{q}{3q+6}\right)}\frac{\sqrt{e_{ij}^\lambda e_{ij}^\lambda}}{2}.$$

15

So, the conformal time derivative of $z_{(s,t)}$ is given by

$$\frac{1}{z_{(s,t)}}\frac{d^2 z_{(s,t)}}{d\eta^2} = \left(\frac{3q+6}{2(m+2)}\right)\left(\left(\frac{3q+6}{2(m+2)}\right)-1\right)\eta^{-2}.$$

Hence, the mode function satisfies the following differential equation

$$\frac{d^2 v_{(s,t)}}{d\eta^2} + \left(c_{(s,t)}^2 k^2 - \frac{1}{z_{(s,t)}}\frac{d^2 z_{(s,t)}}{d\eta^2}\right)v_{(s,t)k} = 0,$$

$$\frac{d^2 v_{(s,t)}}{d\eta^2} + \left(c_{(s,t)}^2 k^2 - \left(\frac{3q+6}{2(m+2)}\right)\left(\left(\frac{3q+6}{2(m+2)}\right)-1\right)\eta^{-2}\right)v_{(s,t)k} = 0,$$

whose solution is

$$v_{(s,t)k}(\eta) = |\eta|^{\frac{1}{2}}\left[c_{(s,t)}^{(1)}(k)\mathcal{H}_v^{(1)}(c_{(s,t)}k|\eta|) + c_{(s,t)}^{(2)}(k)\mathcal{H}_v^{(2)}(c_{(s,t)}k|\eta|)\right], \qquad (31)$$

where $c_{(s,t)}^{(1)}(k)$ and $c_{(s,t)}^{(2)}(k)$ are the integrating constants while $\mathcal{H}^{(1)}$, $\mathcal{H}^{(2)}$ are the Hankle functions of the first and second kind of order $v = \frac{m+2}{2} + \frac{q}{2}$. I have used the Bunch-Davies vacuum by imposing the condition that the mode function approaches the vacuum of the Minkowski spacetime in the short wavelength limit $\frac{b}{k} \ll \frac{1}{H_2}$, where the mode is well with in the horizon. In the rapid oscillation epoch, we have $bH_2 \propto \frac{1}{|\eta|}$ resulting $k\eta \gg 1$. Under this limit, the Bunch-Davies mode function is given by $v_k(\eta) \approx \frac{1}{\sqrt{2c_s k}}e^{-ic_s k\eta}$.

$$v_{(s,t)k}(\eta) = \frac{\sqrt{\pi}}{2}e^{i(v+\frac{1}{2})\frac{\pi}{2}}(-\eta)^{\frac{1}{2}}\mathcal{H}_v^{(1)}(-c_{s,t}k\eta),$$

In the limit, $\frac{k}{bH_2} \to 0$, the asymptotic form of mode function Eq.(31) is given by

$$v_{(s,t)k}(\eta) \to e^{i(\nu+\frac{1}{2})\frac{\pi}{2}}2^{(v-\frac{m+2}{2})}\frac{\Gamma(v)}{\Gamma(\frac{m+2}{2})}\frac{1}{\sqrt{2c_{(s,t)}k}}(-c_{(s,t)}k\eta)^{-v+\frac{1}{2}}. \qquad (32)$$

To obtain scalar power spectrum $P_{(s,t)}^{\frac{1}{2}}(k)$, we use the previous calculated expressions given as

$$P_{(s,t)}^{\frac{1}{2}}(k) = \sqrt{\frac{k^3}{2\pi^2}}\,\left|\frac{v_{(s,t)k}}{z_{(s,t)}}\right|,$$

$$= \sqrt{\frac{k^3}{2\pi^2}}\frac{e^{i(v+\frac{1}{2})\frac{\pi}{2}}}{B_{(s,t)}b(\eta)}2^{(v-\frac{m+2}{2})}\frac{\Gamma(v)}{\Gamma(\frac{m+2}{2})}\frac{1}{\sqrt{2c_{(s,t)}k}}(-c_{(s,t)}k\eta)^{-v+\frac{1}{2}}.$$
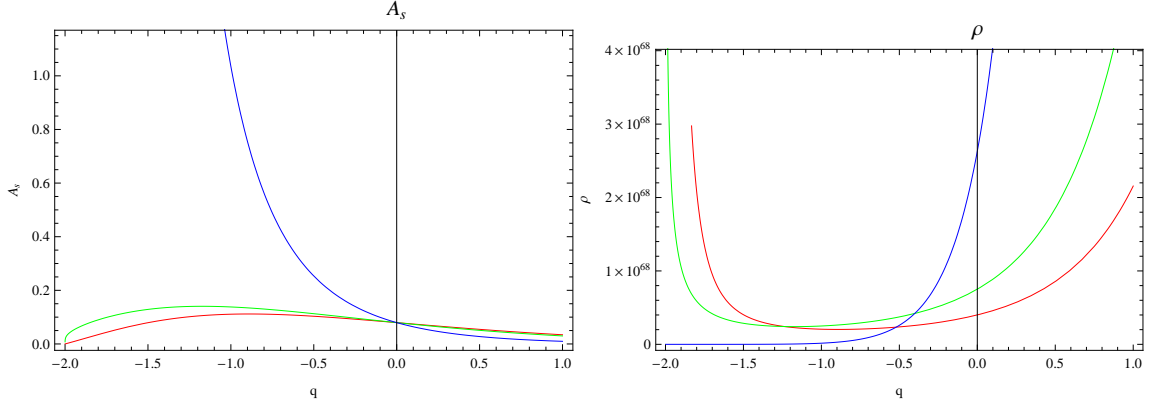
16

Figure 5: (left) The behavior of A_s versus q; (right) ρ versus q are plotted for $m = 1.1$ (red); $m = 2.5$ (green); $m = 10$ (blue).

Rewriting the formula of conformal time in the following form

$$\eta = \int \frac{dt}{b^{\frac{m+2}{3}}(t)} = -\frac{1}{bH_2} + \int \frac{\epsilon db}{b^2 H_2} = -\frac{1}{bH_2}\frac{1}{1-\epsilon}. \tag{33}$$

The last equality in the above equation is obtained by taking the fact that ϵ is constant in the rapid oscillation era. Putting the above value of η, the $P_{(s,t)}$ takes the following form

$$P_{(s,t)}^{\frac{1}{2}}(k) = \frac{k2^{(v-1-\frac{m+2}{2})}}{\sqrt{c_{(s,t)}}\pi B_{(s,t)}b}\frac{\Gamma(v)}{\Gamma(\frac{m+2}{2})}\left(\frac{c_{(s,t)}k}{bH_2(1-\epsilon)}\right)^{-v+\frac{1}{2}}.$$

Moreover, at the horizon crossing scale $c_s k = bH_2$, the power spectrum turned out to be

$$P_{(s,t)}^{\frac{1}{2}}(k) = \frac{2^{(v-1-\frac{m+2}{2})}}{\pi B_{s,t}}\frac{\Gamma(v)}{\Gamma(\frac{m+2}{2})}\frac{H_2}{c_{(s,t)}^{\frac{3}{2}}}(1-\epsilon)^{v-\frac{1}{2}}.$$

To calculate amplitudes related to scalar and tensor spectrum, we write the above expression as

$$P_{(s,t)}^{\frac{1}{2}}(k) = A_{(s,t)}(q)\frac{H_2}{M_p}\mid_{c_{(s,t)}k=bH_2}, \tag{34}$$

17

where

$$A_s(q) = \frac{2^{(v-1-\frac{m+2}{2})}}{\pi B_s c_s} \frac{\Gamma(v)}{\Gamma(\frac{m+2}{2})} (1 - \epsilon_s)^{v-\frac{1}{2}},$$

$$A_s(q) = \frac{2^{(q-\frac{5}{2}+\frac{m+2}{2})}}{\pi(q+2)^{\frac{q}{2}-\frac{1}{2}+\frac{m+2}{2}}} \sqrt{\frac{1 - (\frac{1+2m}{m+2})(\frac{q}{q+2})}{1 - (\frac{1+2m}{m+2})(\frac{q}{3q+6})}} \frac{\Gamma(\frac{m+2}{2}+\frac{q}{2})}{\Gamma(\frac{m+2}{2})},$$

$$A_t(q) = \frac{2^{(q-\frac{5}{2}+\frac{m+2}{2})}}{\pi(q+2)^{\frac{q}{2}-\frac{1}{2}+\frac{m+2}{2}}} \sqrt{\frac{q(m+5)+6(m+2)}{(1 - (\frac{1+2m}{m+2})(\frac{q}{3q+6}))(q(5m+7)+6(m+2))}}$$

$$\times \quad \frac{\Gamma(\frac{m+2}{2}+\frac{q}{2})}{\Gamma(\frac{m+2}{2})}. \tag{35}$$

The above parameters $A_s(q)$, $A_t(q)$ are obtained using the values of v, $B_{(s,t)}$, $c_{(s,t)}$ and ϵ_s in terms of q (defined earlier), corresponding to scalar and power amplitude. To get insight, we have plotted $A_s - q$ in the left panel of Fig. **5** which shows that for all values of $m > 1$, the value of scalar amplitude is always less than unity. Now, we are able to evaluate the energy density using Eqs.(34), (35) and first field equation. As we know that at the earliest stages of the cosmic evolution (not long after the singularity), H_2 and ρ might have been arbitrarily large. It is usually assumed that at densities $\rho \gtrsim M_P^4 \sim 10^{94} g/cm^3$, quantum gravity effects are so significant that quantum fluctuations of the metric exceed the classical value of $g_{\mu\nu}$, and classical space-time does not provide an adequate description of the universe []. Hence, to prove that our model does not lie in quantum gravity regime, we have plotted ρ versus q in the right panel of Fig.**5** for three different values of m. It is clear that there is an increasing behavior among ρ, q and m. An upper bound for anisotropic parameter $1 < m < 45$ is also calculated for which $\rho \lesssim M_P^4 \sim 35.1557 \times 10^{72} (GeV)^4$ in the range $q < 2$.

These quantities lead us to calculate an important physical parameter, i.e., tensor-scalar spectrum ratio, given by

$$r = \frac{P_t}{P_s} = \left(\frac{A_t}{A_s}\right)^2 = \frac{q(m+5)+6(m+2)}{(1 - (\frac{1+2m}{m+2})(\frac{q}{q+2}))(q(5m+7)+6(m+2))}.$$

The behavior of tensor-scalar ratio with respect to q is checked in the left graph of Fig.**6**. The Planck data put an upper bound on the physical parameter r, i.e., $r < 0.11$ (95% C.L.). The graphical analysis (shown in the
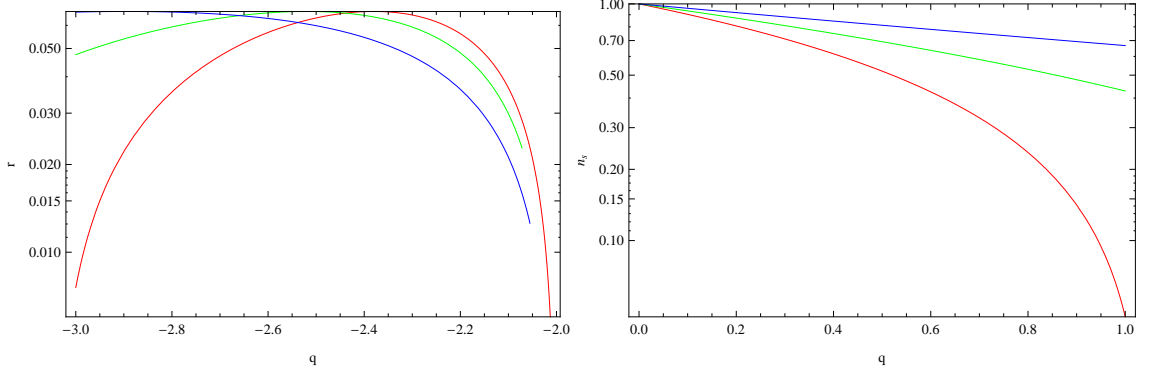
Figure 6: (left) r versus q: for $m = 1.1$ (red); $m = 2.5$ (green); $m = 10^3$ (blue), (right) n_s versus q: for $m = 1.1$ (red); $m = 2.5$ (green); $m = 45$ (blue).

left graph of Fig.**6**) proves that the considered anisotropic model is compatible with recent astrophysical data presented by Planck collaboration for all values of $m \in (1, \infty)$. Moreover, the best fit value of r is obtained in the interval $q \in (-3, -2)$.

Now, we are able to find another parameter, the spectral index (n_s) by the following formula

$$n_s - 1 = \frac{d \ln P_s}{d \ln k} \mid_{c_s k = b H_2} = \frac{d \ln P_s}{dt} \frac{dt}{d \ln k} \mid_{c_s k = b H_2},$$

where

$$\frac{d \ln k}{dt} = \left(\frac{m+2}{3} \right) H_2 \left[1 - \left(\frac{3}{m+2} \right) \epsilon \right].$$

Putting in the above equation, we get n_s in terms of q as follows

$$n_s - 1 = -\frac{6\epsilon}{(m+2) - 3\epsilon} = -\frac{6q}{(m+2)(q+2) - 3q}.$$

The right graph of Fig. **6** proves the compatibility of our anisotropic model with recent Planck astrophysical data, i.e, $n_s = 0.9608 \pm 0.0054$ (68%C.L. or 1σ error). I have plotted n_s versus q for three different values of the anisotropic parameter $m = 1.1$, 2.5, 45, picked from the range of $1 < m < \infty$. It is clear from Fig. **6** (right) that for all these values of m, n_s lies in the range $0 < n_s < 1$. It is also noticed that for $m > 45$, the value of n_s exceeds from unity which is not a physical value. Hence in this case, the model is compatible with Planck data for $1 < m < 45$.

19

4 Concluding Remarks

Recent astrophysical data coming from the Planck satellite verifies that the "large angle anomalies" represent original feature of the cosmic CMB map. This result play a vital role to consider that the "small temperature anisotropies" and "large angle anomalies" may be influenced by anisotropic phase during the early cosmic evolution. This statement has a key importance as it favors to develop an alternative cosmic model to interpret the effects of the early-time universe on the current structure of large scale without affecting the processes of nucleosynthesis. Warm inflation is a good model for LSS formation, in which the density fluctuations arise from thermal fluctuation. It is described by a damping factor in the inflaton's equation of motion. The magnitude of this factor suggests the prospect that it has the strong effect prolonging inflation.

Motivated by this fact, I study the warm inflation with non-minimal derivative coupling model (which solves the issue of few number of e-folds and clear the scenario "how reheating occurs?") during rapid oscillations. To get the comprehensive results, I have used the framework of homogeneous but anisotropic LRS BI cosmic model, which is asymptotically equivalent to the standard FRW universe. I reconstruct the formalism of oscillatory inflation using anisotropic background. A power law form of potential is used to find the adiabatic index (γ) and time period of the oscillations. On solving these equations, I am able to calculate a constraint on the amplitude of the inflaton (Φ) during non-minimal case for the realization of inflation. To check the validity of the inequality in anisotropic model, I have plotted trajectories of $\Phi^{\frac{q+2}{2}}$ and the expression on right hand side (say f) of Eq.(12) versus q for specified values of m in the left and right panel of Fig.**1**, respectively. It is very much clear from the comparison of left and right graph of Fig.**1** that the value of $\Phi^{\frac{q+2}{2}}$ is much less than the expression f for $q < 2$ and $m > 1$.

The end of inflation is discussed by using a special form of Damour-Mukhanov potential where the inflation continues whenever $d < g(\mathfrak{b}, q)$ (given in 20). The violation of this inequality (i.e., $d = g(\mathfrak{b}_{end}, q)$ and $d > g(\mathfrak{b}(t > t_{end}), q)$), inflation terminates. The graphical analysis of this double valued function is shown in Fig. **2** for three different values of $\mathfrak{b} = 1$ (red), 5 (green) 10 (blue). It is observed that $g(\mathfrak{b}, q)$ has an increasing behavior for all values of $\mathfrak{b} > 0$ in the range $q \in (-\infty, 1)$. The point of intersection of the three curves is $(1, 0)$, so inflation ends for $d > 1$ and $d \simeq 1$ ($\phi \sim \phi_c$). Further, I calculate the number of e-folds for the minimal

and non-minimal case during high friction regime. The plot for $\mathcal{N} - q$ is presented to set an upper bound on $\mathcal{N}_{min}$, by fixing $\Phi_{end} \sim 10^{-17} m_P$ (left panel) and $\Phi_{end} \sim 10^{-6} m_P$ (right panel) and varying $m = 1.5,\ 2.5,\ 10$ in Fig.**3**. It is noticed from both graphs of Fig.**3** that an increment in the scale of Φ_{end} leads to decrease the value of $\mathcal{N}_{min}$ while an increasing relationship exists between $\mathcal{N}$ and m. The theory may become more viable at least in the context of perturbations generation as the anisotropic model has ability to provide more number of e-folds ($\mathcal{N} > 8.4$) in non-minimal case as compared to the minimal case.

Moreover, the cosmological perturbation scheme is developed in the anisotropic background using the Mukhanov-Sasaki equation during rapid oscillation era. The explicit expressions are calculated for speed of sound, scalar and tensor power spectrum, tensor to scalar ratio and spectral index. Figure **4** shows that the speed of sound lies in the feasible range $0 < c_s < 1$ for all values of $m > 0$. To get insight, we have plotted $A_s - q$ in the left panel of Fig. **5** which shows that for all values of $m > 1$, the value of scalar amplitude is always less than unity. Hence, to prove that our model does not lie in quantum gravity regime, we have plotted ρ versus q in the right panel of Fig.**5** for three different values of m. It is clear that there is an increasing behavior among ρ, q and m. An upper bound for anisotropic parameter $1 < m < 45$ is also calculated for which $\rho \lesssim M_P^4 \sim 35.1557 \times 10^{72} (GeV)^4$ in the range $q < 2$. The behavior of tensor-scalar ratio with respect to q is checked in the left graph of Fig.**6**. The left graph of Fig.**6** proves that the considered anisotropic model is compatible with recent astrophysical data presented by Planck collaboration for all values of $m \in (1, \infty)$. Moreover, the best fit value of r is obtained in the interval $q \in (-3, -2)$. n_s versus q is plotted for three different values of the anisotropic parameter $m = 1.1,\ 2.5,\ 45$, picked from the range of $1 < m < \infty$ in Fig.**6** (right). It is clear from graphical analysis that for all these values of m, n_s lies in the range $0 < n_s < 1$. It is also noticed that for $m > 45$, the value of n_s exceeds from unity which is not a physical value. Hence in this case, the model is compatible with Planck data for $1 < m < 45$.

It is worth mentioned that all the results reduced to the isotropic case for $m = 1$ [15]. The major difference is that it is not possible to find the exact value of the parameter q during anisotropic background. In future, I will perform this type of study by considering thermal correction to the effective potential, also the temperature dependency of the dissipative factor and checking all consistency conditions.

References

[1] Guth, A.: Phys. Rev. D **23**(1981)347.

[2] Starobinsky, A.A.: Phys. Lett. B **91**(1980)99.

[3] Liddle, A. and Lyth, D.: *Cosmological Inflation and Large-Scale Structure*, (Cambridge University Press, 2000).

[4] Linde, A.: *Particle Physics and Inflationary Cosmology* (Harwood, Chur, Switzerland, 1990).

[5] Tolman, R.C.: *Relativity, Thermodynamics and Cosmology* (Clarendon Press, Oxford, 1934).

[6] Khoury, J., Ovrut, B.A., Steinhardt, P.J. and Turok, N.: Phys. Rev. D **64**(2001)123522; Khoury, J., Ovrut, B.A., Seiberg, N., Steinhardt, P.J. and Turok, N.: Phys. Rev. D **65**(2002)086007; Steinhardt, P.J. and Turok, N.: Science **296**(2002)1436; Phys. Rev. D **65**(2002)126003.

[7] Kanekar, N., Sahni, V. and Shtanov, Y.: Phys. Rev. D **63**(2001)083520.

[8] Damour, T. and Mukhanov, V.F.: Phys. Rev. Lett. **80**(1998)3440.

[9] Liddle, A. and Mazumder, A.: Phys. Rev. D **58**(1996)083508.

[10] Bartruma, S., Gilb, M., Bereraa, A., Cerezob, R., Ramosc, R.O. and Rosa, J.G.: Phys. Lett. B **732**(2014)116.

[11] Taruya, A.: Phys. Rev. D **59**(1999)103505.

[12] Lee, J., Koh, S., Park, C., Sin, S.J. and Lee, C.H.: Phys. Rev. D **61**(1999)027301.

[13] Sami, M.: Grav. Cosmol. **8**(2003)309.

[14] Sushkov, S.V.: Phys. Rev. D **80**(2009)103505; Saridakis, E., Sushkov, S.V.: Phys. Rev. D **81**(2010)083510; Sadjadi, H.M.: Phys. Rev. D **83**(2011)107301; Yang, N., Gao, Q. and Gong, Y.: Int. J. Mod. Phys. A **30**(2015)1545004; Cai, Y. and Piao, Y.S.: J. High Eener. Phys. **03**(2016)134; Huang, Y. and Gong, Y.: Sci. China Phys. Mech. Astron. **59**(2016)640402.

[15] Sadjadi, H.M. and Goodarzi, P.: Phys. Lett. B **732**(2014)278.

[16] Russell, E., Kilinc, C.B. and Pashaev, O.K.: Mon. Not. R. Astron. Soc. **442**(2014)2331.

[17] Sharif, M. and Saleem, R.: Eur. Phys. J. C **74**(2014)2738; Astropart. Phys. **62**(2015)100.

[18] Bezrukov, F.L. and Shaposhnikov, M.E.:Phys. Lett. B **659**(2008)703; Bezrukov, F., Magnin, A., Shaposhnikov, M. and Sibiryakov, S.: J. High Energ. Phys. **01** (2011)016.

[19] Germani, C. and Kehagias, A.: Phys. Rev. Lett. **105**(2010)011302.

[20] Collins, C.B.: Phys. Lett. A **60**(1977)397; Sharif, M. and Zubair, M.: Astrophys. Space Sci. **330**(2010)399.

[21] Shtanov, Y., Traschen, J. and Brandenberger, R.: Phys. Rev. D **51**(1995)5438.

[22] Sami, M.: Gravit. Cosmol. **8**(2003)309.

[23] Ade, P.A.R. et al.: arXiv:1403.3985; arXiv:1403.4302.

[24] Germani, C. and Watanabe, Y. J. Cosmol. Astropart. Phys. **031**(2011)1107.

[25] Germani, C., Martucci, L. and Moyassari, P.: Phys. Rev. D **85**(2012)103501.